J. Chem. Sci. Vol. 129, No. 1, January 2017, pp. 9–20. © Indian Academy of Sciences.
DOI 10.1007/s12039-016-1213-y

REGULAR ARTICLE

Self-assembly, structures and properties of three new Ni(II) coordination polymers derived from two different bis-pyridyl-bis-amide ligands and two aromatic polycarboxylates

HONGYAN LIN*, JUNJUN SUN, GUOCHENG LIU*, XIANG WANG and PANWEN CHEN
Department of Chemistry, Bohai University, Jinzhou 121000, People's Republic of China
Email: linhongyan_2005@126.com; lgch1004@sina.com

MS received 14 July 2016; revised 24 September 2016; accepted 21 November 2016

Abstract. Three new Ni(II) coordination polymers exhibiting different 1D and 2D framework structures have been hydrothermally synthesized: $[Ni(L^1)(1,3\text{-BDC})(H_2O)_3]\cdot H_2O$ (**1**), $[Ni(L^1)(1,3,5\text{-HBTC})(H_2O)_3]$ (**2**), $[Ni_3(L^2)_3(1,3,5\text{-BTC})_2(H_2O)_8]\cdot 12H_2O$ (**3**) [L^1 = N,N′-bis(pyridin-3-yl)cyclohexane-1,4-dicarboxamide, L^2 = N,N′-bis(3-pyridyl)octandiamide, 1,3-H_2BDC = 1,3-benzenedicarboxylic acid, 1,3,5-H_3BTC = 1,3,5-benzenetricarboxylic acid]. X-ray single crystal diffraction analyses revealed that polymer **1** is a 2D interlaced layer based on the 1D $[Ni(L^1)(1,3\text{-BDC})(H_2O)_3]$ meso-helical chains. Polymer **2** is a 1D wave-shaped chain derived from the 1D $[Ni(L^1)]_n$ chain and monodentate coordinated 1,3,5-HBTC anions. Polymer **3** possesses an interesting 2D layer containing the trinuclear $[Ni_3(1,3,5\text{-BTC})_2]$ substructural unit and 1D zigzag $[Ni(L^2)]_n$ chain, representing a 3,4-connected $\{6\cdot 8^2\}_2\{6^2\cdot 8^2\cdot 10\cdot 12\}$ topology. Finally, the adjacent 1D chains or the 2D layers are connected through hydrogen bonding interactions to construct 3D supramolecular networks. Further, the thermal stability, solid state fluorescent property and photocatalytic activity of **1–3** have been investigated.

Keywords. Metal-organic coordination polymer; crystal structure; bis-pyridyl-bis-amide ligand; fluorescence; photocatalysis

1. Introduction

Metal-organic coordination polymers (MOCPs) represent an interesting new research field and attracted significant attention in recent years.[1–4] Up to now, a great number of MOCPs possessing diverse structures (such as 1D infinite chains, 2D layers and 3D networks) have been proven to be potential functional materials for luminescence, catalysis, gas storage and separation, magnetism, ion exchange and so on.[5–8] During the process of self-assembly of metal ions and organic bridging ligands, many influencing factors may play important roles and even change the final structures of the aimed MOCPs, such as the geometric requirement of the metal ions, the geometrical configuration of the organic ligands, the system pH, the category of solvent and the reaction temperature.[9–13] So, significant interest has arisen in the structural tuning of MOCPs by rational design and selection of organic bridging ligands, usually including O-donor and N-donor ligands.[14–18] Wherein, the mixed-ligand systems consisting of N-donor heterocyclic ligands and O-donor carboxylate ligands have been widely used to obtain MOCPs.[19–23] For example, Wen *et al.* have prepared four Cd(II)/Cu(II) coordination polymers derived from a multidentate triazole ligand and two different dicarboxylates $[Cd(3,3'\text{-tmbpt})(1,4\text{-BDC})]\cdot 2.5H_2O$, $[Cd(3,3'\text{-tmbpt})(1,3\text{-BDC})]\cdot 21\text{-}H_2O$, $[Cu(3,3'\text{-tmbpt})(1,3\text{-BDC})]\cdot H_2O$ and $[Cu(3,3'\text{-tmbpt})(1,3\text{-BDC})]\cdot 2H_2O$ (3,3′-tmbpt = 1-((1H-1,2,4-triazol-1-yl)methyl)-3,5-bis(3-pyridyl)-1,2,4-triazole, 1,4-H_2 1,3-BDC = 1,4-benzenedicarboxylic acid, 1,3-H_2BDC = 1,3-benzenedicarboxylic acid).[24]

More recently, the bis-pyridyl-bis-amide ligands have been introduced into metal-carboxylate systems and a number of MOCPs with interesting properties have been generated, due to their several advantages: (a) As neutral nitrogen-/oxygen-donor ligands, both the pyridine moieties and the amide groups of these ligands can coordinate with metal ions; (b) The conformational changes of these ligands can meet the requirements of the coordination geometries of metal ions, which is conducive to construct new complexes more easily; (c) The amide groups could function not only as hydrogen bonding acceptors but also as hydrogen bonding donors, which may generate high-dimensional supramolecular networks. For example, Chen *et al.*, have reported a series of Zn(II)/Cd(II) coordination polymers derived from the flexible bis-pyridyl-bis-amide and aromatic polycarboxylates mixed ligands,

*For correspondence

all of them exhibiting fluorescence property.[25–28] Our group has also made some efforts in constructing the Cu(II)/Co(II)/Cd(II) coordination polymers containing the flexible/rigid bis-pyridyl-bis-amide ligands and polycarboxylates, and studied their electrochemical, photocatalytic or fluorescence properties.[29–32] However, the related Ni(II) coordination polymers constructed by the flexible/rigid bis-pyridyl-bis-amide ligands and aromatic polycarboxylates are still limited, up to now.[29,33] Therefore, two bis-pyridyl-bis-amide ligands [L^1, N,N′-bis(pyridin-3-yl)cyclohexane-1,4-dicarboxamide; L^2, N,N′-bis(3-pyridyl)octandiamide] have been selected as the main ligands and combined with two polycarboxylates [1,3-H_2BDC, 1,3,5-H_3BTC (1,3,5-benzenetricarboxylic acid)] to construct Ni(II) coordination polymers, aiming to study their effect on the final architectures and potential properties of target MOCPs. In this paper, we report three new Ni(II) MOCPs based on the mixed-ligands of two different bis-pyridyl-bis-amide (L^1, L^2) and two aromatic polycarboxylates (1,3-H_2BDC, 1,3,5-H_3BTC), namely, $[Ni(L^1)(1,3\text{-BDC})(H_2O)_3]\cdot H_2O$ (**1**), $[Ni(L^1)(1,3,5\text{-HBTC})(H_2O)_3]$ (**2**) and $[Ni_3(L^2)_3(1,3,5\text{-BTC})_2(H_2O)_8]\cdot 12H_2O$ (**3**). Polymer **1** represents the first 2D interlaced layer based on the 1D $[Ni(L^1)]_n$ *meso*-helical chains constructed from the bis-pyridyl-bis-amide ligand.

2. Experimental

2.1 *Materials and methods*

The main ligands L^1 and L^2 were synthesized by the literature method.[34,35] The ancillary ligand 1,3-H_2BDC and 1,3,5-H_3BTC were commercially obtained from Aladdin Reagent Co. (China) and used without further purification. All other reagents and solvents for syntheses were purchased from commercial sources and were used without further purification. FT-IR spectrum (in KBr pellet) was performed on a Varian FT-IR 640 spectrometer. Thermogravimetric (TG) data of three title polymers were taken on a Pyris-Diamond thermal analyzer under nitrogen atmosphere. Powder X-ray diffraction (PXRD) investigation was recorded on a Bruker AXS D8-Advanced diffractometer. The fluorescence spectra were carried out using a HITACHI F–4500 Fluorescence Spectrophotometer. UV-Vis absorption spectra were taken on a SP-1900 spectrophotometer.

2.2 *Preparation of the polymers*

2.2a *Synthesis of $[Ni(L^1)(1,3\text{-BDC})(H_2O)_3]\cdot H_2O$ (**1**)*: A mixture of $Ni(NO_3)_2\cdot 6H_2O$ (0.058 g, 0.2 mmol), 1,3-H_2BDC (0.025 g, 0.15 mmol), L^1 (0.033 g, 0.10 mmol), H_2O (12 mL) and NaOH (0.018 g, 0.45 mmol) was stirred for 30 min, then transferred and sealed in a 25 mL Teflon reactor, which was heated at 120°C and kept for 4 days; then cooled to room temperature leading to the formation of green block crystals for polymer **1**. Suitable crystals were manually picked, washed with water and dried in air. Yield: ∼42% (based on Ni). Anal. Calcd. for $C_{26}H_{32}NiN_4O_{10}$ (619.27): C 50.38, H 5.21, N 9.04%. Found: C 50.45, H 5.13, N 9.17%. IR (KBr pellet, cm^{-1}): 3460 (s), 3205 (m), 3008 (w), 2365 (w), 2338 (w), 2092 (w), 1689 (s), 1600 (s), 1527 (s), 1481 (s), 1434 (s), 1381 (s), 1321 (m), 1281 (m), 1201 (w), 1115 (w), 989 (w), 876 (m), 810 (s), 748 (m), 715 (s), 635(w), 556 (m), 523 (w).

2.2b *Synthesis of $[Ni(L^1)(1,3,5\text{-HBTC})(H_2O)_3]$ (**2**)*: Polymer **2** was synthesized in the same way as **1**, except that 1,3,5-H_3BTC (0.032 g, 0.15 mmol) was used instead of 1,3-H_2BDC (0.025 g, 0.15 mmol). Green block-shaped crystals suitable for X-ray single diffraction of **2** were isolated (yield: 36% based on Ni). Anal. Calcd. for $C_{27}H_{30}N_4NiO_{11}$ (645.26): C 50.21, H 4.69, N 8.68%. Found: C 50.14, H 4.75, N 8.56%. IR (KBr pellet, cm^{-1}): 3437 (s), 3248 (m), 3111 (w), 2361 (w), 1721 (m), 1617 (s), 1565 (s), 1519 (m), 1473 (w), 1428 (s), 1388 (m), 1362 (s), 1264 (w), 1219 (m), 1153 (s), 1101 (s), 990 (w), 932 (w), 873 (w), 808 (m), 729 (s), 690 (w), 664 (m), 612 (m), 592 (w), 540 (w), 508 (w).

2.2c *Synthesis of $[Ni_3(L^2)_3(1,3,5\text{-BTC})_2(H_2O)_8]\cdot 12H_2O$ (**3**)*: The method for polymer **3** was the same as for **2**, except that L^2 (0.033 g, 0.10 mmol) was used instead of L^1 (0.033 g, 0.10 mmol). Green crystals of **3**, suitable for single X-ray diffraction were obtained by mechanical separation from the amorphous solid in 35% yield (based on Ni). Anal. Calcd. for $C_{72}H_{112}Ni_3N_{12}O_{38}$ (1929.87): C 44.77, H 5.85, N 8.71%. Found: C 44.69, H 5.73, N 8.88%. IR (KBr pellet, cm^{-1}): 3420 (s), 3126 (m), 2932 (w), 2355 (w), 2079 (w), 1679 (w), 1615 (s), 1533 (s), 1484 (s), 1434 (s), 1378 (s), 1253 (w), 1190 (s), 1158 (m), 1108 (m), 933 (m), 807 (m), 764 (m), 701 (s), 645 (w), 613 (w), 526 (w).

2.3 *X-ray crystallography*

X-ray diffraction data for polymers **1–3** were collected on a Bruker Smart Apex-II CCD area detector and graphite-monochromated Mo Kα (λ = 0.71073 Å) by ω and θ scan mode. All the structures were solved by direct methods and refined on F^2 by full-matrix least-squares methods using the SHELXS program of the SHELXTL package. For polymers **1–3**, the crystal parameters, data collection, and refinement results are summarized in Table 1. Selected bond distances and bond angles are listed in Table S1–S3 (Supplementary Information). Hydrogen bonding geometries of polymers **1–3** are summarized in Table S4 (Supplementary Information).

3. Results and Discussion

3.1 *Description of crystal structure of $[Ni(L^1)(1.3\text{-BDC})(H_2O)_3]\cdot H_2O$ (**1**)*

Single-crystal X-ray diffraction analysis reveals that polymer **1** is monoclinic crystal system with *C 2/c*

Table 1. Crystal data and structure refinement for polymers **1–3**.

Formula	$C_{26}H_{32}NiN_4O_{10}$	$C_{27}H_{30}N_4NiO_{11}$	$C_{72}H_{112}Ni_3N_{12}O_{38}$
Formula wt.	619.27	645.26	1929.87
Cryst. size, mm^3	0.23 × 0.21 × 0.16	0.22 × 0.18 × 0.14	0.23 × 0.21 × 0.20
Crystal system	Monoclinic	Monoclinic	Triclinic
Space group	C 2/c	P 21/c	P -1
T, k	293(2)	296(2)	296(2)
a, Å	25.893(5)	14.700(3)	9.2271(5)
b, Å	16.974(5)	12.017(2)	11.7044(7)
c, Å	13.924(5)	16.197(3)	22.0100(14)
α, deg	90	90	83.4150(10)
β, deg	110.486(5)	99.359(4)	83.3690(10)
γ, deg	90	90	70.9440(10)
V, $Å^3$	5733(3)	2822.9(9)	2224.2(2)
Z	8	4	1
D_{calc}, g/cm^3	1.430	1.518	1.441
μ, mm^{-1}	0.738	0.756	0.723
	2576	1344	1016
F(000)	1.430	1.518	1.441
hkl range	$-32 \le h \le +21$	$-18 \le h \le +19$	$-9 \le h \le +11$
	$-19 \le k \le +21$	$-15 \le k \le +15$	$-13 \le k \le +15$
	$-12 \le l \le +17$	$-15 \le l \le +21$	$-28 \le l \le +24$
θ_{max}, deg	26.19	27.95	27.47
R_{int}	0.0265	0.0528	0.0194
R_1^a	0.0398	0.0943	0.0511
wR_2^b(all data)	0.1056	0.2987	0.1475
GOF	1.033	1.058	1.019
$\Delta\rho_{max}$, e $Å^{-3}$	0.679	2.005	0.769
$\Delta\rho_{min}$, e $Å^{-3}$	−0.243	−0.859	−0.643

$^aR_1 = \Sigma||F_o| - |F_c||\Sigma|F_o|$; $^bwR_2 = \Sigma[w(F_o^2–F_c^2)^2]/\Sigma[w(F_o^2)^2]^{1/2}$.

space group, which shows a 2D interlaced layer derived from a 1D polymeric chain $[Ni(L^1)(1,3\text{-BDC})(H_2O)_3]_n$. The asymmetric unit of **1** contains one Ni(II) ion, an L^1 ligand, one 1,3-BDC anion, three coordinated water molecules and one lattice water molecule. Each Ni(II) ion is six-coordinated by two pyridyl nitrogen atoms [Ni(1)–N(1) = 2.133(2) Å, Ni(1)–N(3)#1 = 2.145(2) Å] from two separate L^1 ligands, one carboxyl oxygen atom O(6) of a 1,3-BDC anion with distance of 2.0430(18) Å, and three oxygen atoms [O(1W), O(2W) and O(3W)] belonging to three coordinated water molecules [Ni(1)–O distances: 2.042(2)–2.085(2) Å] to complete a distorted octahedral geometry (Figure 1a). In complex **1**, the L^1 ligands adopt only one μ_2-bridging coordination mode (via ligation of pyridyl nitrogen atoms), but they exhibit two kinds of conformations (L^{1a} and L^{1b}, Table 2) due to the flexibility of the cyclohexyl group. For each kind of the L^1 ligands, their two pyridine rings are parallel. The ligands L^{1a} and L^{1b} alternately are connected to the adjacent Ni(II) ions to construct a 1D $[Ni(L^1)]$ meso-helical chain with alternate iteration of left-handed and right-handed half turns (Figure 1b, 1c and Figure S1a in Supplementary Information), in which only one carboxyl group of the 1,3-BDC anion adopts a monodentate coordination mode hanging on the side of the 1D chain. In the 1D chain, the different non-bonding Ni···Ni distances are 18.23 Å (L^{1a}) and 18.16 Å (L^{1b}).

Interestingly, the adjacent 1D meso-helical chains are in mutually staggered arrangement to form the interlaced layer (Figure 1d, 1e and Figure S1b in Supplementary Information). Further, there exist strong O–H···O hydrogen bonding interactions [O(1W)–H(1WA)···O(1) = 2.764(3) Å O(2W)–H(2WA)···O(2) = 2.689(4) Å, Table S4 in Supplementary Information] among the adjacent chains in the interlaced layer to consolidate the 2D framework (Figure S1c in Supplementary Information). To the best of our knowledge, the polymer **1** represents the first 2D interlaced layer based on the 1D $[Ni(L^1)]_n$ *meso*-helical

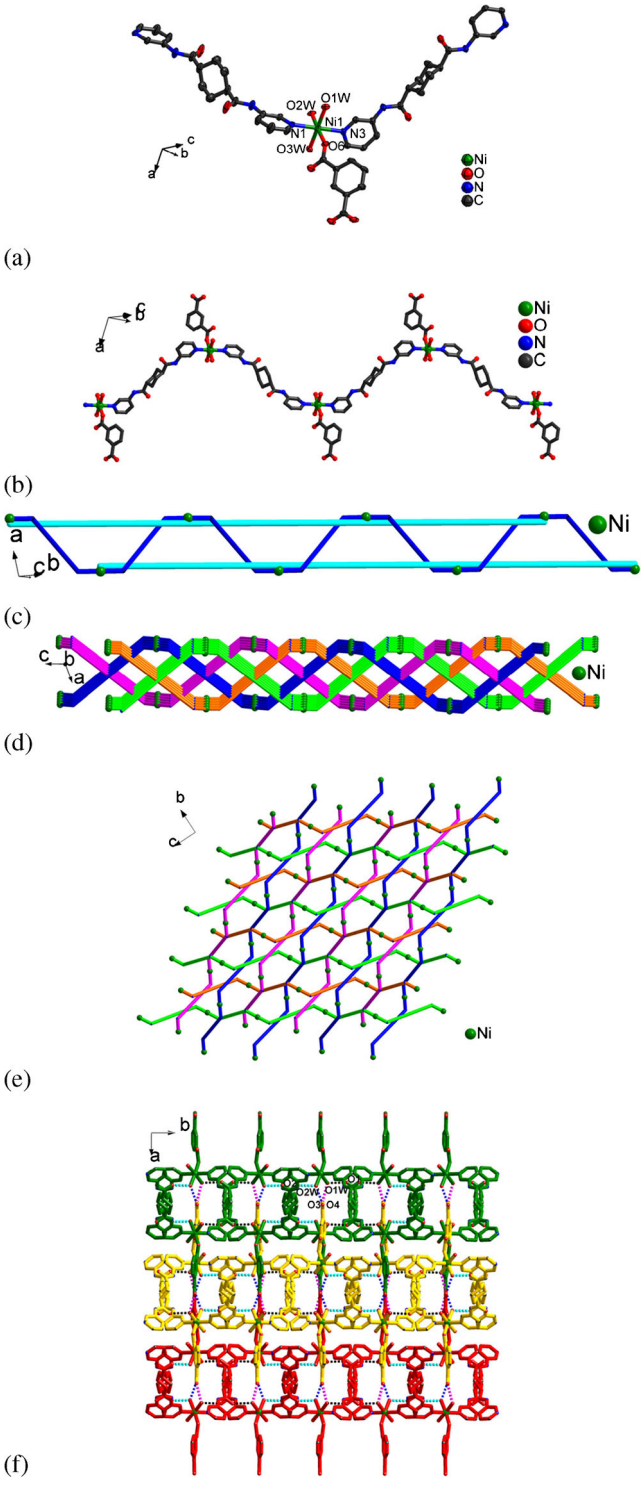

Figure 1. (a) The coordination environment of Ni(II) ion in polymer **1**. (b) The 1D [Ni(L^1)(BDC)(H_2O)$_3$] *meso*-helical chain. (c) The simplified representation of 1D chain of **1**. (d) The simplified representation of the interlaced arrangement of the adjacent 1D chains along the b-axis in **1**. (e) View of the interlaced 2D framework of **1**. (f) The 3D supramolecular network of **1** formed by hydrogen bonding interactions along the c-axis.

chains derived from the bis-pyridyl-bis-amide ligand. Finally, the 2D interlaced layers are extended into a 3D supramolecular network by the O–H···O hydrogen bonding interactions [O(1W)–H(1WA)···O(4) = 2.694(3) Å, O(2W)–H(2WA)···O(3) = 2.676(3) Å], as shown in Figure 1f.

3.2 *Description of crystal structure of [Ni(L^1)(1,3,5-HBTC)(H_2O)$_3$] (2)*

Similar to polymer **1**, using 1,3,5-H_3BTC in the reaction, polymer **2** was successfully prepared. It crystallizes in monoclinic crystal system with *P21/c* space group. The asymmetric unit of **2** consists of one Ni(II) ion, one L^1 molecule, one 1,3,5-HBTC anion and three coordinated water molecules. As shown in Figure 2a, Ni(II) ion displays a six-coordinated distorted octahedral geometry, coordinated by one carboxyl oxygen atom from 1,3,5-HBTC anion with Ni(1)–O(1) distance of 2.039(5) Å, two pyridyl nitrogen atoms from two L^1 ligands [Ni(1)–N(1) = 2.119(6) Å, Ni(1)–N(2)#1 = 2.148(6) Å], and three oxygen atoms of three coordinated water molecules [Ni(1)–O(1W) = 2.062(5) Å, Ni(1)–O(2W) = 2.076(5) Å, Ni(1)–O(3W) = 2.033(5) Å]. In polymer **2**, the adjacent Ni(II) ions are linked by L^1 ligands with a μ_2-bridging mode to form a 1D [Ni(L^1)] wave-like chain (Figure 2b), in which the 1,3,5-HBTC anions only adopt a monodentate mode and hang on both sides of the 1D chain. In **2**, the L^1 exhibits only one coordination conformation, which bridges two Ni(II) ions with the non-bonding Ni···Ni distance as 18.08 Å, and the dihedral angle between its two pyridine rings is 7.39° (Table 2). Furthermore, the 1D chains are connected by the O–H···O hydrogen bonding interactions between the coordinated water molecules and the carbonyl group of L^1 ligands [O(1W)–H(1WA)···O(7), 3.008(10) Å; O(2W)–H(2WB)···O(8), 2.757(8) Å] to give a 2D supramolecular structure, as shown in Figure S2a (Supplementary Information). The π-π stacking interactions between the pyridyl rings among the L^1 ligands consolidate the 2D supramolecular architecture of **2** [the shortest centroid–centroid distance is 3.678(5) Å]. Finally, the other O–H···O hydrogen bonding interactions [O(1W)–H(1WA)···O(5) = 3.228(9) Å, O(3W)–H(3WA)···O(2) = 2.755(8) Å, O(1W)–H(1WB)···O(4) = 2.718(8) Å, O(3W)–H(3WB)···O(3) = 2.641(8) Å] between the coordinated water molecules and the carboxyl oxygen of 1,3,5-HBTC anions link the neighboring 2D layers to form a 3D supramolecular network (Figure 2c). The hydrogen bonding data are summarized in Table S4 (Supplementary Information).

Table 2. Coordination modes of Ni(II) ions, the bis-pyridyl-bis-amide ligands (L^1, L^2) and polycarboxylates (1,3-BDC, 1,3,5-HBTC, 1,3,5-BTC) in polymers **1**–**3**.

Polymers	Ni(II) ion(s)	Polycarboxylates	Bis-pyridyl-bis-amide ligands	Dihedral angle of pyridyl rings
1		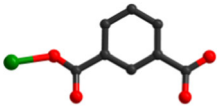	 **L^{1a}** Ni1···Ni1 distance: 18.23 Å	0°
			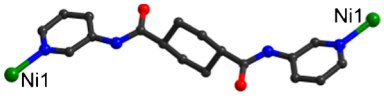 **L^{1b}** Ni1···Ni1 distance: 18.16 Å	0°
2		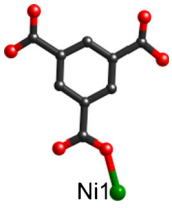	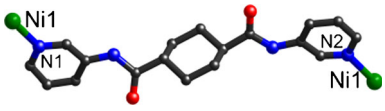 Ni1···Ni1 distance: 18.08 Å	7.39°
3	 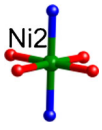	 Ni1···Ni1 distance: 7.91	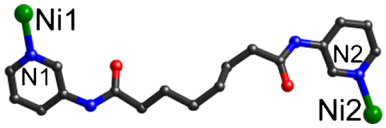 **L^{2a}** Ni1···Ni1 distance: 17.56 Å	35.60°
			 **L^{2b}** Ni1···Ni1 distance: 18.72 Å	0°

3.3 *Description of crystal structure of $[Ni_3(L^2)_3(1,3,5\text{-}BTC)_2(H_2O)_8]\cdot 12H_2O$ (3)*

Polymer **3** was obtained by a similar procedure as that of **2**, except that L^2 was used instead of L^1. X-ray diffraction analysis displays that polymer **3** possesses a 2D coordination framework in triclinic crystal system with *P-1* space group. The asymmetric unit of **3** contains three Ni(II) ions, two 1,3,5-BTC anions, three L^2 molecules, eight coordinated water molecules and twelve lattice water molecules. As shown in Figure 3a, there are two crystallographically independent Ni(II) ions in **3**. The Ni1 ion is six-coordinated by two carboxyl oxygen atoms from two different 1,3,5-BTC anions [Ni(1)–O(1), Ni(1)–O(1)#1, 2.0392(18) Å], two pyridyl nitrogen atoms from two L^2 molecules [Ni(1)–N(1), Ni(1)–N(1)#1, 2.140(2) Å] and two coordinated water molecules [Ni(1)–O(1W), Ni(1)–O(1W)#1, 1.979(2) Å], showing a distorted octahedral geometry. The Ni2 ion is also in six-coordinated distorted octahedral geometry, surrounded by one carboxyl oxygen atom of a 1,3,5-BTC anion [Ni(2)–O(3) = 2.0630(19) Å], two pyridyl nitrogen atoms of two L^2 molecules [Ni(2)–N(2) = 2.112(2) Å,

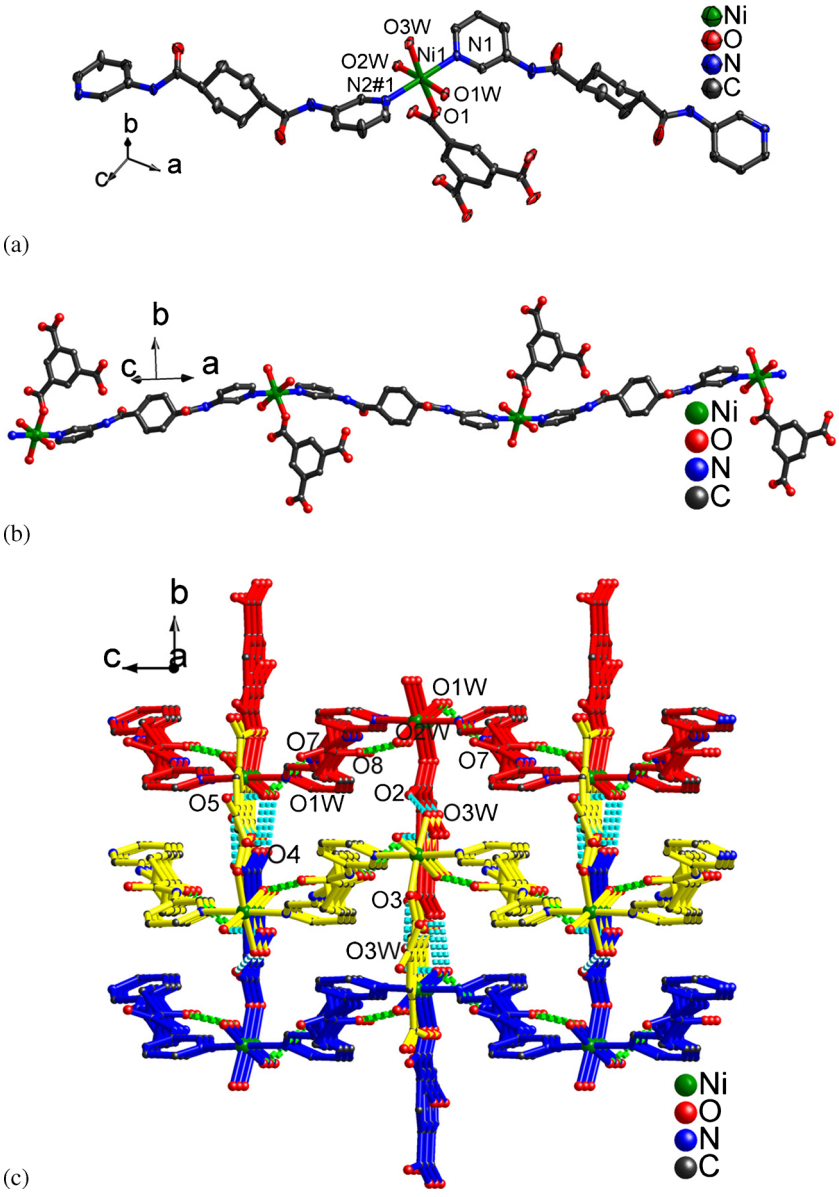

Figure 2. (a) The coordination environment of Ni(II) ion in polymer **2**. (b) The 1D polymeric chain of **2**. (c) The 3D supramolecular structure of **2** formed by hydrogen bonding interactions.

Ni(2)–N(5) = 2.111(2) Å] and three oxygen atoms belonging to three coordinated water molecules [Ni(2)–O(2W) = 2.0552(19) Å, Ni(2)–O(3W) = 2.091(2) Å, Ni(2)–O(4W) = 2.052(2) Å]. Each 1,3,5-BTC anion adopts a monodentate-monodentate bridging mode (Table 2) to connect with two Ni(II) ions with the non-bonding Ni1···Ni2 distance of 7.91 Å. Two Ni2 and one Ni1 ions are bridged by two 1,3,5-BTC anions to build a trinuclear [Ni_3(1,3,5-BTC)$_2$] substructural unit, as shown in Figure S3a (Supplementary Information). Then, the trinuclear structural units are further connected by μ_2-bridging L^2 ligands to generate a 2D polymeric layer (Figure 3b). Wherein, the ligands show two different coordination conformations (L^{2a} and L^{2b}, Table 2). The ligands L^{2a} and L^{2b} alternately link the adjacent Ni(II) ions to construct a 1D [Ni(L^2)] chain (Figure S3b in Supplementary Information). Ni1 and Ni2 ions are bridged by the L^{2a} ligand with the non-bonding distance of 17.56 Å, while two Ni2 ions are linked through the L^{2b} ligand [Ni2··Ni2 = 18.72 Å]. In the 2D of **3**, each Ni1 is surrounded by two L^2 ligands and two 1,3,5-BTC anions, which can be regarded as a four-connected node; while Ni2 is linked by one 1,3,5-BTC anion and two L^2 ligands, which can be considered as a three-connected node. The 1,3,5-BTC anion acts as a two-connector to link two Ni(II) ions, then the L^2

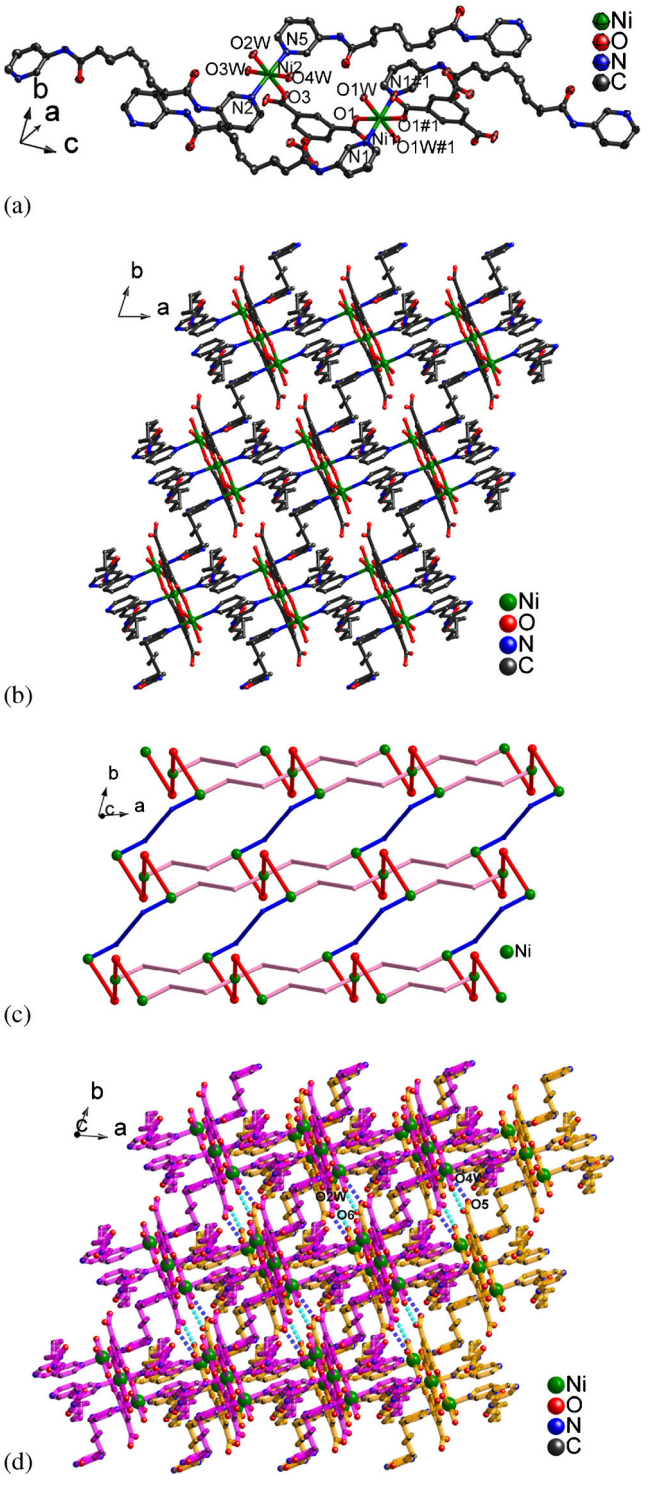

Figure 3. (a) The coordination environment of Ni(II) ions in polymer **3**. (b) The 2D polymeric layer of **3**. (c) The schematic representation of the 2D layer in **3**. (d) The 3D supramolecular structure for **3** formed by hydrogen bonding interactions.

ligand serves as a linker, thus the resulting 2D layer of **3** is an interesting 2,3,4-connected framework with point symbol of $\{6.8^2\}_2\{6^2.8^2.10.12\}\{6\}_2$ (Figure 3c). In addition, such 2D polymeric layers are further connected through the hydrogen bonding interactions between the coordinated water molecules and the carboxyl oxygen atoms of 1,3,5-BTC anions [O(2W)–H(2WB)$\cdots$O(6) = 2.711(3) Å, O(4W)–H(4WB)$\cdots$O(5) = 2.746(3) Å], giving a 3D supramolecular network (Figure 3d and Figure S3d in Supplementary Information).

3.4 *Powder X-ray diffraction of polymers **1–3***

The powder X-ray diffraction (PXRD) patterns of the as-synthesized crystal materials were almost identical to that calculated from the single-crystal structures, as shown in Figure S7–S9 (Supplementary Information). The diffraction peaks of the simulated and experimental patterns match well in key positions, indicating the phase purities of the as-synthesized polymers **1–3**.

3.5 *Thermal stability analyses of polymers **1–3***

The thermogravimetric (TG) curves of polymers **1–3** were determined in the temperature range of 20–700°C with a heating rate of 10°C·min^{-1}, as shown in Figures S10–S12 (Supplementary Information). The TG curve of polymer **1** displays two obvious weight loss steps. The first weight loss step in the region of 155–255°C should be ascribed to the loss of lattice water and coordinated water molecules (11.63%, calcd. 11.43%). The second weight loss step in the range of 370–510°C is equivalent to the decomposition of organic ligands (1,3-BDC and L^1). The final remaining weight (12.36%) is close to 12.23% by assuming NiO phases as the final residue (calcd 12.06%), indicating this is the final product. For the TG curve of polymer **2**, the first weight loss occurs about 160°C, which can be assigned to the loss of coordinated water molecules (8.86%, calcd. 8.37%). Then the framework of **2** began to decompose with a continuous weight loss up to 550°C, and the remaining weight 11.76% is in agreement with the percentage of Ni and O components (calcd. 11.58%). For **3**, its TG curve shows three weight loss steps, the first step should be attributed to the loss of lattice water molecules (10.56%, calcd. 11.19%), the second step could be attributed to the loss of coordinated water molecules (7.27%, calcd. 7.46%), and the third step might be ascribed to the loss of organic ligands. And the remaining weight 12.20% is in consistent with the Ni and O components in NiO (calcd. 11.61%), indicating that the final product is NiO.

3.6 *Fluorescent property of polymers **1–3***

The fluorescent property of polymers **1–3**, the free ligands L^1 and L^2 were studied at room temperature in the

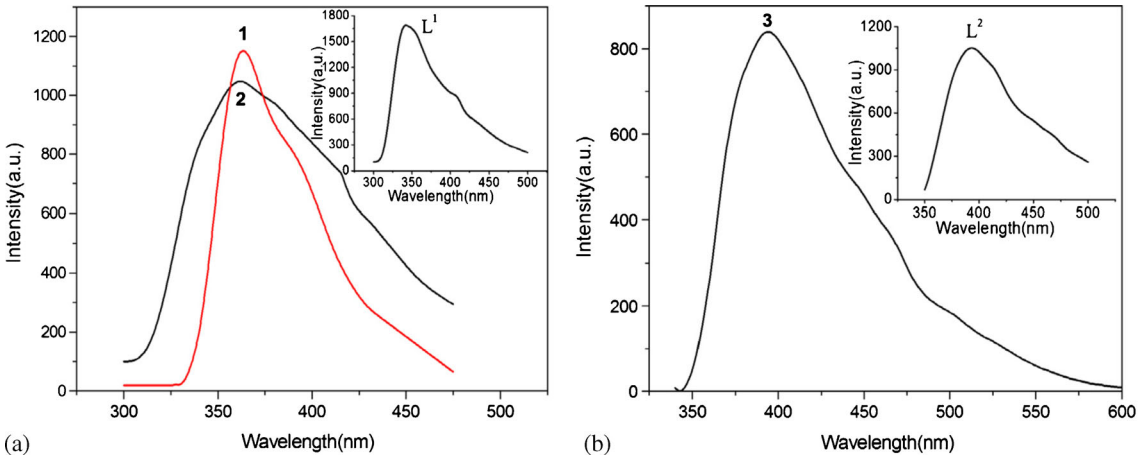

Figure 4. (a) The emission spectra of polymers **1** and **2** and the free ligand L^1 ($\lambda_{ex} = 280$ nm). (b) The emission spectrum of polymer **3** and the free ligand L^2 ($\lambda_{ex} = 280$ nm).

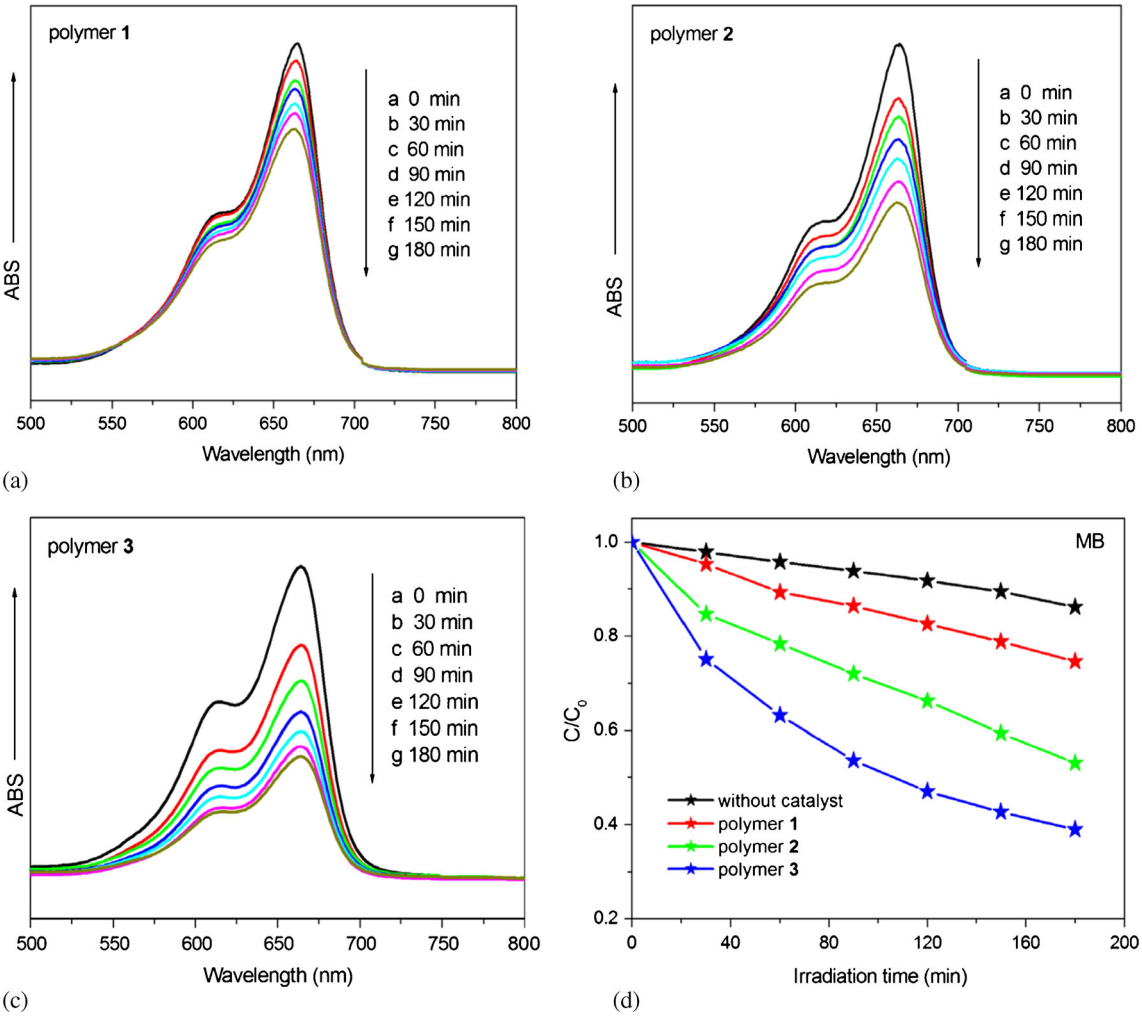

Figure 5. (a–c) Absorption spectra of the MB solution ($10.0\,mg{\cdot}L^{-1}$) during the decomposition reaction under UV irradiation in the presence of polymers **1**–**3**. (d) Photocatalytic decomposition rates of MB solution under UV irradiation with the use of polymer catalysts **1**–**3** and without catalyst under the same conditions.

solid state (Figure 4). The solid-state 1,3-H_2BDC and 1,3,5-H_3BTC ligands can exhibit fluorescence at room temperature, but its fluorescent emission resulting from the $\pi^* \rightarrow$n transition is very weak compared to that of the $\pi^* \rightarrow \pi$ transition of the N-donor ligands L^1 and L^2; so, 1,3-H_2BDC and 1,3,5-H_3BTC ligands almost have no contribution to the fluorescent emission of the title polymers.[36,37] As shown in Figure 4a, the free ligand L^1 displays the emission peak at 348 nm for the excitation at 280 nm. The polymers **1–2** and L^1 ligands have similar emission spectra, and their emission bands are observed at 363 nm for **1** and 360 nm for **2** (λ_{ex} = 280 nm). The red shift of 15 nm for **1** and 12 nm for **2** were seen, which may be ascribed to metal-to-ligand or ligand-to-metal charge-transfer transitions.[38,39] The free ligand L^2 has the emission peak at 390 nm for the excitation at 280 nm, and polymer **3** exhibits the emission band at 395 nm (Figure 4b). Three title polymers may be the potential candidates for photoactive materials due to their high thermal stability and insolubility in common organic solvents.

3.7 *Photocatalytic property of polymers **1–3***

Recently, some metal-organic coordination polymers have been used as one kind of photocatalysts for decomposing organic pollutants under UV irradiation.[40,41] Herein, we studied the photocatalytic activities of polymers **1–3** for the photodegradation of organic dye contaminants methylene blue (MB) and rhodamine B (RhB) under UV irradiation to evaluate the photocatalytic effectiveness in the purification of waste water. The photocatalytic performance of polymers **1–3** for the degradation of MB and RhB was studied by a typical process: 90 mg of the title polymers as powder was dispersed in the MB or RhB solution (10.0 mg·L^{-1}),

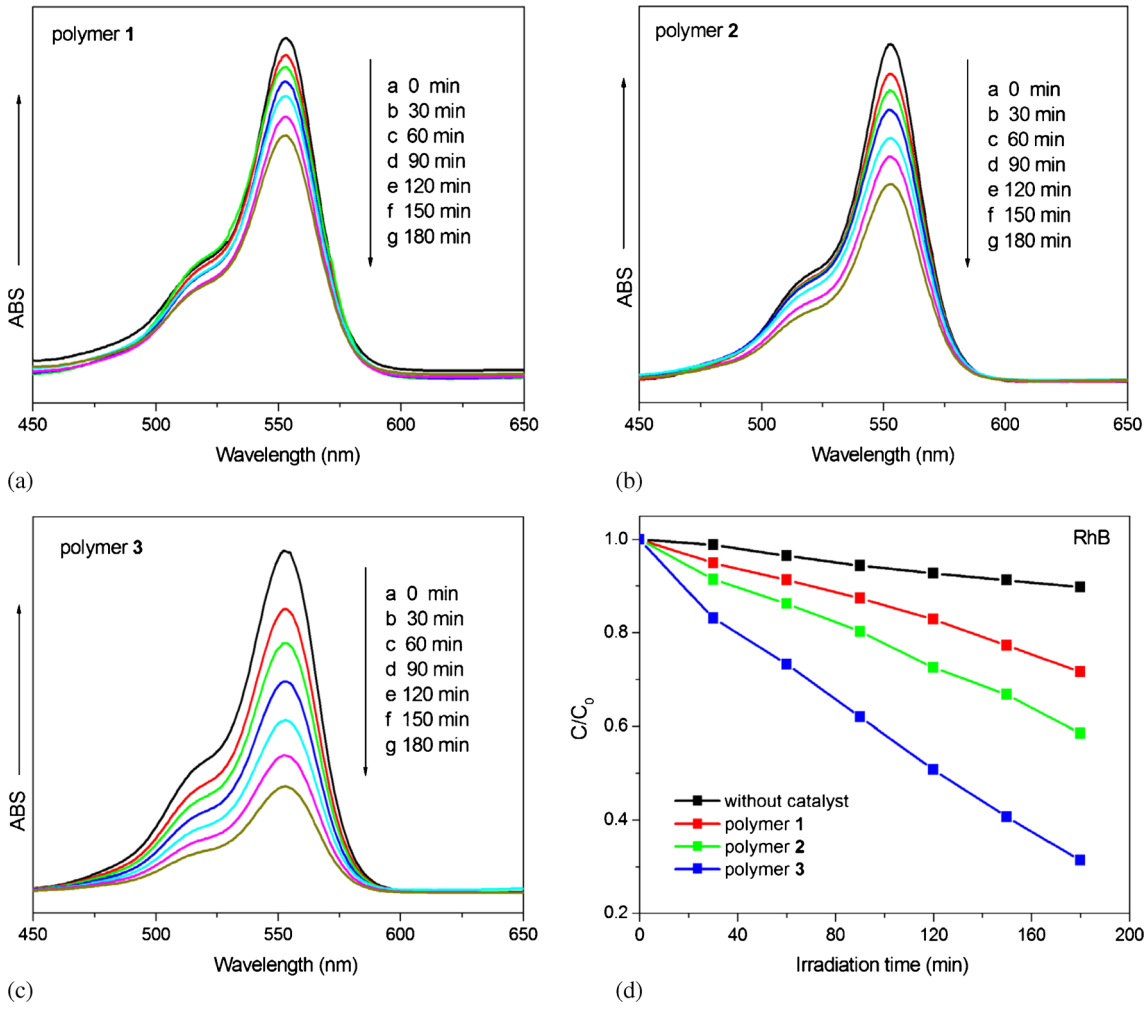

Figure 6. (a–c) Absorption spectra of the RhB solution (10.0 mg·L^{-1}) during the decomposition reaction under UV irradiation with the presence of polymers **1–3**. (d) Photocatalytic decomposition rates of RhB solution under UV irradiation with the use of polymer catalysts **1–3** and without catalyst under the same conditions.

and then magnetically stirred in the dark for 30 min to ensure equilibrium of the working solution. The dye solution was then exposed to UV irradiation from a 125 W Hg lamp and kept continuously stirred. Every 30 min interval, 3.0 mL of MB or RhB solution sample was taken out for analysis. As shown in Figure 5, in the presence of title polymers, the absorption peaks of MB decreased with time under UV irradiation. In addition, the concentration of MB and RhB (C) versus reaction time (t) are plotted in Figure 5d. It can be seen that the photocatalytic activity increased from 14% (without any catalyst) to 28% for **1**, 47% for **2** and 62% for **3** after 180 min of UV irradiation. Similar experiments were performed to study the photocatalytic activity of three title polymers on the degradation of RhB (Figure 6). From the Figure 6d, we find that the degradation of RhB in 180 min irradiation are 30% for **1**, 42% for **2** and 70% for **3**. The different structures of polymers may lead to the discrepancy in the band-gap sizes, which will affect their final photocatalytic activities.[31,42] In this paper, polymer **3** shows the highest photocatalytic activity for the degradation of MB and RhB.

4. Conclusions

In summary, three new Ni(II) coordination polymers were successfully synthesized under hydrothermal conditions by the assembly of two different bis-pyridyl-bis-amide ligands and two aromatic polycarboxylates. Three polymers possess versatile coordination features: a 2D interlaced layer derived from the 1D chains for **1**, a 1D wave-shaped chain for **2**, and a 2D coordination framework for **3**. The structural differences reveal that two bis-pyridyl-bis-amide ligands and two different polycarboxylates have modulating effect on the final architectures of polymers. Further, the fluorescent and the photocatalytic properties of the three title polymers were studied, and the experimental results imply that these polymers may be good candidates for fluorescent and photocatalytic materials.

Supplementary Information (SI)

X-ray crystallographic data for polymers **1**–**3** reported in this paper have been deposited in the Cambridge Crystallographic Data Center with CCDC reference numbers CCDC 1041874 for **1**, 1435170 for **2** and 1435171 for **3**. These data can be obtained free of charge from The Cambridge Crystallographic Data Centre *via* www.ccdc.cam.ac.uk/data_request/cif. The tables of selected bond lengths and angles, the related hydrogen bonding geometries of polymers **1**–**3** (Tables S1–S4), and additional figures (structural figures, IR spectra, PXRD and TG curves, Figures S1–S12) are available in Supplementary Information; see, www.ias.ac.in/chemsci.

Acknowledgements

This work was supported by the National Natural Science Foundation of China (No. 21471021, 21501013, 21401010), New Century Excellent Talents in University (NCET-09-0853) and Program of Innovative Research Team in University of Liaoning Province (LT2012020).

References

1. Qin J H, Ma L F, Hu Y and Wang L Y 2012 Syntheses, structures and photoluminescence of five zinc(II) coordination polymers based on 5-methoxyisophthalate and flexible N-donor ancillary ligands *CrystEngComm* **14** 2891
2. Yoon M, Srirambalaji R and Kim K 2012 Homochiral Metal–Organic Frameworks for Asymmetric Heterogeneous Catalysis *Chem. Rev.* **112** 1196
3. Moon H R, Lim D W and Suh M P 2013 Fabrication of metal nanoparticles in metal–organic frameworks *Chem. Soc. Rev.* **42** 1807
4. Gai Y L, Jiang F L, Xiong K C, Chen L, Yuan D Q, Zhang L J, Zhou K and Hong M C 2012 Temperature-Dependent in Situ Reduction of 4,4′-Azobispyridine via Solvothermal Reaction *Cryst. Growth Des.* **12** 2079
5. Liu B, Zhao R L, Yang G P, Hou L, Wang Y Y and Shi Q Z 2013 Two isostructural amine-functionalized 3D self-penetrating microporous MOFs exhibiting high sorption selectivity for CO_2 *CrystEngComm* **15** 2057
6. Liu Y Y, Li J, Ma J F, Ma J C and Yang J 2012 A series of 1D, 2D and 3D coordination polymers based on a 5-(benzonic-4-ylmethoxy)isophthalic acid: Syntheses, structures and photoluminescence *CrystEngComm* **14** 169
7. Suh M P, Park H J, Prasad T K and Lim D W 2012 Hydrogen Storage in Metal–Organic Frameworks *Chem. Rev.* **112** 782
8. Cui Y J, Yue Y F, Qian G D and Chen B L 2012 Luminescent Functional Metal–Organic Frameworks *Chem. Rev.* **112** 1126
9. Li Y W, Li D C, Xu J, Hao H G, Wang S N, Dou J M, Hu T L and Bu X H 2014 Structural modulation in two Cu^{II}-based MOFs by synergistic assembly involving the mixed-ligand synthetic strategy and the solvent effect *Dalton Trans.* **43** 15708
10. Li M, Liu L, Zhang L, Lv X, Ding J, Hou H and Fan Y 2014 Novel coordination polymers of Zn(II) and Cd(II) tuned by different aromatic polycarboxylates: Synthesis, structures and photocatalytic properties *CrystEngComm* **16** 6408
11. Tian D, Li Y, Chen R Y, Chang Z, Wang G Y and Bu X H 2014 A luminescent metal–organic framework demonstrating ideal detection ability for nitroaromatic explosives *J. Mater. Chem.* **2** 1465

12. Liu H Y, Yang J, Liu Y Y and Ma J F 2012 pH-dependent assembly of two inorganic–organic hybrid compounds based on octamolybdates: An unusual intercalated layer and a 3D 4-connected framework *Dalton Trans.* **41** 9922
13. Gao Q, Xie Y B, Li J R, Yuan D Q, Yakovenko A A, Sun J H and Zhou H C 2012 Tuning the Formations of Metal–Organic Frameworks by Modification of Ratio of Reactant, Acidity of Reaction System, and Use of a Secondary Ligand *Cryst. Growth Des.* **12** 281
14. Gu J Z, Kirillov A M, Wu J, Lv D Y, Tang Y and Wu J C 2013 Synthesis, structural versatility, luminescent and magnetic properties of a series of coordination polymers constructed from biphenyl-2,4,4′-tricarboxylate and different N-donor ligands *CrystEngComm* **15** 10287
15. Hong D H and Suh M P 2014 Enhancing CO_2 Separation Ability of a Metal–Organic Framework by Post-Synthetic Ligand Exchange with Flexible Aliphatic Carboxylates *Chem. Eur. J.* **20** 426
16. He Y B, Zhou W, Krishna R and Chen B L 2012 Microporous metal–organic frameworks for storage and separation of small hydrocarbons *Chem. Commun.* **48** 11813
17. Brozek C K and Dincă M 2014 Cation exchange at the secondary building units of metal–organic frameworks *Chem. Soc. Rev.* **43** 5456
18. Zhang H, Jiang W, Yang J, Liu Y Y, Song S and Ma J F 2014 Four coordination polymers constructed by a novel octacarboxylate functionalized calix[4]arene ligand: syntheses, structures, and photoluminescence property *CrystEngComm* **16** 9939
19. Zhang H M, Yang J, Liu Y Y, Kang D W and Ma J F 2015 A family of coordination polymers assembled with a flexible hexacarboxylate ligand and auxiliary N-donor ligands: Syntheses, structures, and physical properties *CrystEngComm* **17** 3181
20. Fan L M, Zhang X T, Sun Z, Zhang W, Ding Y S, Fan W L, Sun L M, Zhao X and Lei H 2013 Ancillary Ligands Dependent Structural Diversity of A Series of Metal–Organic Frameworks Based on 3,5-Bis(3-carboxyphenyl)pyridine *Cryst. Growth Des.* **13** 2462
21. Lin L, Yu R M, Yang W B, Wu X Y and Lu C Z 2012 A Series of Chiral Metal–Organic Frameworks Based on Oxalyl Retro-Peptides: Synthesis, Characterization, Dichroism Spectra, and Gas Adsorption *Cryst. Growth Des.* **12** 3304
22. Cheng P C, Kuo P T, Liao Y H, Xie M Y, Hsu W and Chen J D 2013 Ligand-Isomerism Controlled Structural Diversity of Zn(II) and Cd(II) Coordination Polymers from Mixed Dipyridyladipoamide and Benzenedicarboxylate Ligands *Cryst. Growth Des.* **13** 623
23. Liu S J, Xue L, Hu T L and Bu X H 2012 Two new Co^{II} coordination polymers based on carboxylate-bridged di- and trinuclear clusters with a pyridinedicarboxylate ligand: Synthesis, structures and magnetism *Dalton Trans.* **41** 6813
24. Kan W Q, Wen S Z, Hu H Y and Kan Y H 2015 Cd(II) and Cu(II) coordination polymers based on aultidentate N-donor ligand: Syntheses, crystal structures, optical band gaps, and photoluminescence *J. Coord. Chem.* **68** 2492
25. Sie M J, Chang Y J, Cheng P W, Kuo P T, Yeh C W, Cheng C F, Chen J D and Wang J C 2012 Interpenetrated and polycatenated nets of Cd(II) coordination networks from mixed N, N'-dipyridyladipoamide and dicarboxylate ligands *CrystEngComm* **14** 5505
26. Cheng J J, Chang Y T, Wu C J, Hsu Y F, Lin C, Proserpio D and Chen J D 2012 Highly interpenetrated diamondoid nets of Zn(II) and Cd(II) coordination networks from mixed ligands *CrystEngComm* **14** 537
27. Cheng P C, Wu M H, Xie M Y, Huang W J, He H Y, Wu T T, Lo Y C, Proserpio D M and Chen J D 2013 Construction of N, N'-di(3-pyridyl)adipoamide-based Zn(II) and Cd(II) coordination networks by tuning the isomeric effect of polycarboxylate ligands *CrystEngComm* **15** 10346
28. Cheng P C, Kuo P T, Xie M Y, Hsu W and Chen J D 2013 Structure-directing roles of auxiliary polycarboxylate ligands in the formation of Zn(II) and Cd(II) coordination polymers based on a flexible N, N'-di(3-pyridyl)dodecanediamide *CrystEngComm* **15** 6264
29. Wang X L, Luan J, Lin H Y, Xu C, Liu G C, Zhang J W and Tian A X 2013 The design and construction of a series of metal–organic coordination polymers based on two isomericsemi-rigid bis-pyridyl-bis-amide ligands and three aromatic polycarboxylates *CrystEngComm* **15** 9995
30. Wang X L, Luan J, Sui F F, Lin H Y, Liu G C and Xu C 2013 Structural Diversities and Fluorescent and Photocatalytic Properties of a Series of Cu^{II} Coordination Polymers Constructed from Flexible Bis-pyridyl-bis-amide Ligands with Different Spacer Lengths and Different Aromatic Carboxylates *Cryst. Growth Des.* **13** 3561
31. Wang X L, Luan J, Lin H Y, Lu Q L, Le M, Liu G C and Shao J Y 2014 Metal(II)–Organic Coordination Polymers Modulated by Two Isomeric Semirigid Bis-Pyridyl–Bis-Amide Ligands: Structures, Fluorescent Sensing Behavior, and Selective Photocatalysis *ChemPlusChem* **79** 1691
32. Wang X L, Sui F F, Lin H Y, Zhang J W and Liu G C 2014 Multifunctional Cobalt(II) Coordination Polymers Tuned by Flexible Bis(pyridylamide) Ligands with Different Spacers and Polycarboxylates *Cryst. Growth Des.* **14** 3438
33. Wang X L, Luan J, Lin H Y, Xu C and Liu G C 2013 Three multifunctional three-dimensional metal–organic frameworks based on a flexible N,N0-bis(3-pyridinecarboxamide)-1,6-hexane and 3-nitrophthalate: Syntheses, structures and properties *Inorg. Chim. Acta* **408** 139
34. Muthu S, Yip J H K and Vittal J J 2002 Coordination networks of Ag(I) and N, N'- bis(3-pyridinecarboxamide)-1,6-hexane: Structures and anion exchange *J. Chem. Soc. Dalton Trans.* **31** 4561
35. Hsu Y F, Hsu W, Wu C J, Cheng P C, Yeh C W, Chang W J, Chen J D and Wang J C 2010 Roles of halide anions in the structural diversity of Zn(II) complexes containing the flexible N,N′-di(4-pyridyl)adipoamide ligand *CrystEngComm* **12** 702

36. Shi X, Zhu G S, Fang Q, Wu G, Tian G, Wang R, Zhang D, Xue M and Qiu S L 2004 Novel Supramolecular Frameworks Self-Assembled from One-Dimensional Polymeric Coordination Chains *Eur. J. Inorg. Chem.* **2004** 185
37. Shi X, Zhu G S, Wang X H, Li G H, Fang Q R, Zhao X J, Wu G, Tian G, Xue M, Wang R W and Qiu S L 2005 Polymeric Frameworks Constructed from a Metal-Organic Coordination Compound, in 1-D and 2-D Systems: Synthesis, Crystal Structures, and Fluorescent Properties *Cryst. Growth Des.* **5** 341
38. Hsu Y F, Hu H L, Wu C J, Yeh C W, Proserpioc D M and Chen J D 2009 Ligand isomerism-controlled structural diversity of cadmium(II) perchlorate coordination polymers containing dipyridyladipoamideligands *CrystEngComm* **11** 168
39. Sun G M, Huang H X, Tian X Z, Song Y M, Zhu Y, Yuan Z J, Xu W Y, Luo M B, Liu S J, Feng X F and Luo F 2012 Carboxylate-assisted acylamide metal–organic frameworks: Synthesis, structure, thermostability and luminescence studies *CrystEngComm* **14** 6182
40. Lv J, Lin J X, Zhao X L and Cao R 2012 Photochromic hybrid materials of cucurbituril and polyoxometalates as photocatalysts under visible light *Chem. Commun.* **48** 669
41. Gong Y, Wu T and Lin J H 2012 Metal–organic frameworks based on naphthalene-1,5-diyldioxy-di-acetate: Structures, topologies, photoluminescence and photocatalytic properties *CrystEngComm* **14** 3727
42. Guo J, Yang J, Liu Y Y and Ma J F 2012 Two novel 3D metal–organic frameworks based on two tetrahedral ligands: Syntheses, structures, photoluminescence and photocatalytic properties *CrystEngComm* **14** 6609